Applying Kramers formula for the nuclear fission problem: how accurate is it?

I I Gontchar, N E Aktaev, A L Litnevsky, E G Pavlova

Omsk State Transport University, Prospekt Marxa, 35, 644046 Omsk, Russia

E-mail: vigichar@hotmail.com, lusha.85@mail.ru

Abstract. We compare results of dynamical modeling of the fission process with predictions of the Kramers formulas. For the case of large dissipation these are two: the integral rate R_I and its approximation R_O. As the ratio of the fission barrier height B_f to the temperature T, ε, reaches 4, any analytical rate is expected to agree with the dynamical quasistationary value R_D within 2%. We perform modeling using several potentials and find that the difference between the R_O and the R_D sometimes exceeds 20% even for $\varepsilon > 4$. Such discrepancy is not acceptable nowadays because it is comparable to the quantum, non-markovian and multidimensional effects. The features of the potentials which cause this disagreement are identified and studied. It is demonstrated that this is the R_I, not the R_O, which meets the expectation above irrespectively of the potential profile.

25.70.Jj,25.70.-z

1. Introduction

The statistical model of the fission process was introduced by Bohr and Wheeler [1]. Soon after this Kramers derived several formulas for the decay rate [2]. One of those is widely used in modern nuclear physics. Alternative way is to calculate the quasistationary fission rate (QSFR) by means of solving numerically the stochastic differential equations [3]. Both the Kramers and the dynamical approaches are based on the picture of Brownian motion. The dynamical approach is more accurate but very time consuming. The difference between the Kramers fission rates and the QSFR was shown to reach approximately 20% [4 – 6]. One the other hand, in the pioneering work [7] good agreement between a Kramers rate and the QSFR was demonstrated.

This discrepancy was acceptable twenty years ago. Nowadays there are several circumstances which require more accurate analytical description of the fission rate (FR). These are: i) the quantum correction to the Kramers formula [8]; ii) the contribution of the non-markovian effects [9] and iii) the multidimensionality of the fission process [10].

Many aspects of the problem can be responsible for the significant difference between the Kramers fission rates and the QSFR, e.g. the deformation dependence of the friction (inertia) tensor and of the single-particle level density parameter, the approximations made in the derivation of the Kramers formulas, the non-harmonic character of the collective potential. The aims of the present study are i) to disentangle the effects of the potential in the accuracy of the Kramers formulas reducing the uncertainties related to all other parameters and ii) to find a way for diminishing the discrepancy between the analytical and dynamical rates down to about 2%. This value is comparable with the statistical errors of the QSFR achievable during a reasonable time of computer modeling.

This is an ambitious program, therefore only the one-dimensional overdamped motion of a Brownian particle representing the fission process is considered below. Moreover, the deformation dependence of the friction, inertia and level density parameters is ignored. These serious restrictions, however, are still being used in modern studies [11, 12].

2. Dynamical modeling

We restrict ourselves with the symmetric fission at zero angular momentum. The nucleus shape is characterized by the half distance between mass centers of the nascent fragments over the radius of the spherical nucleus, q. Initially all the nuclei are assumed to be concentrated at the quasistationary point $q_{qs} = 0.375$. We deliberately position the saddle ($q_{sd} = 1.2$) and the scission ($q_{sc} = 3.0$) points as well as q_{qs} far from each other to exclude possible influence of the distance between them onto our results.

Within our approximations, the nuclear collective motion is modeled using the Euler scheme for the stochastic (Langevin) equations [3]:

$$q_{n+1} = q_n - \frac{\tau}{m\beta}\left(\frac{dU}{dq}\right)_n + b_n\sqrt{\frac{T\tau}{m\beta}} \quad . \tag{1}$$

Here β is the damping coefficient and m is the inertia parameter; the time step of dynamical modeling is denoted by τ; b_n is a Gaussian random number with a variance of 2. The temperature T is calculated using the Fermi-gas relation at the quasistationary point $T = \sqrt{E^*_{tot}/a}$ and is supposed to be deformation-independent. In this work $\beta = 10\ zs^{-1}$ has been chosen.

Within the framework of the Langevin formalism, the time-dependent FR, R_f, can be calculated by counting the number of trajectories N_f which reach the scission point before the time moment t:

$$R_f(t) = \frac{1}{N_{tot} - N_f(t)}\frac{dN_f(t)}{dt} \quad . \tag{2}$$

Here N_{tot} is the total number of trajectories. The R_f is close to zero when t is small. Then it increases with t and reaches its quasistationary value R_D. This is illustrated by Fig. 1.

3. Analytical formulas for the fission rate and representation of results

The Kramers formulas, the accuracy of which we are studying here, read

$$R_I = \frac{T}{m\beta}\left\{\int_{-\infty}^{q_{sd}} \exp\left[-\frac{U(y)}{T}\right]dy \int_{q_{qs}}^{q_{sc}} \exp\left[\frac{U(x)}{T}\right]dx\right\}^{-1}; \qquad R_O = \frac{\omega_{qs}\omega_{sd}}{2\pi\beta}\exp\left(-\frac{B_f}{T}\right). \tag{3, 4}$$

In these equations ω_{sd} and ω_{qs} are the absolute values of the angular frequencies of the collective motion around the maximum (q_{sd}) and the minimum (q_{qs}) of the potential energy $U(q)$. Eq. (3) is supposed to be valid if i) $B_f T^{-1} >> 1$ and ii) β is large enough, i.e. $\beta \geq \max(\omega_{qs}, \omega_{sd})$.

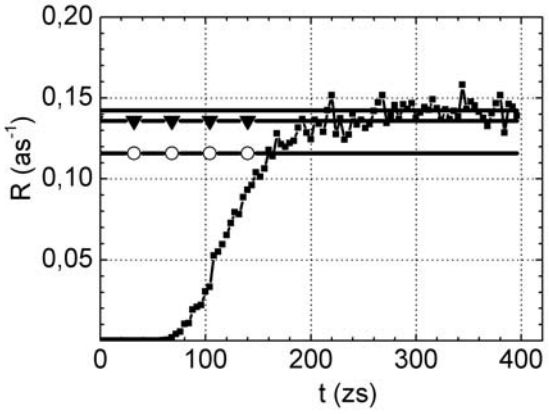

Figure 1. The fission rates versus time. The oscillating line with boxes corresponds to the R_f, the R_D (solid line), the R_O (open circles) and the R_I (closed triangles) are also shown. These calculations have been performed for the W-potential (see below) at $\varepsilon = 3.8$

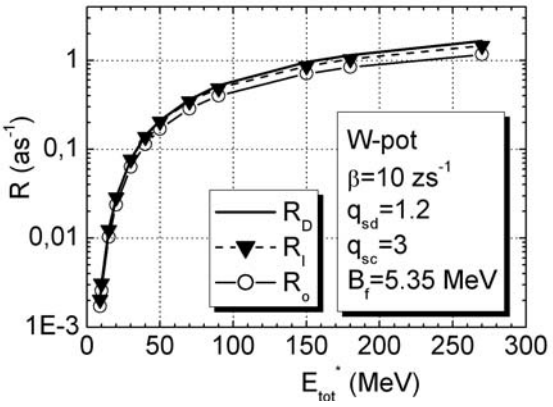

Figure 2. The fission rates versus E_{tot}^{*}. All notations are as in Fig. 1

Eq. (4) results from Eq. (3) by extending the upper integral limits to plus infinity, the q_{qs} to minus infinity and by expanding $U(q)$ in the integrands up to quadratic terms in $(q-q_{qs})$ and $(q-q_{sd})$. Thus Eq. (4) is valid under the additional requirements: iii) q_{sc} is far enough from q_{sd} and iv) $U(q)$ is represented by two parabolas with the stiffnesses C_{sd} and C_{qs} near its extremes.

Of the two Kramers fission rates, R_I and R_O, the former is expected to agree better to the R_D.These three rates versus excitation energy E_{tot}^{*} are shown in Fig. 2. They cover 3 orders of magnitude and are hardly distinguishable. Therefore it is convenient to characterize the deviation of a fission rate R_{ik} from another rate R_{jk} (both calculated with the same potential k) by means of the fractional difference $\xi_{ijk} = \left(R_{ik} - R_{jk}\right)/R_{jk}$. For instance the fractional difference between R_{OH} and R_{DH} reads ξ_{ODH} and $\xi_{ODH} = 5\%$ means that in the case of H-potential (see below) the overdamped Kramers rate calculated using Eq. (4) exceeds the dynamical QSFR by 5%.

For the convenience of the reader we collect in Table 1 the values of the parameters used in the present calculations.

Table 1. The values of the parameters used in the present calculations.

B_f, MeV	m, MeV·zs^2	τ, zs	a, MeV^{-1}	q_{qs}	q_{sd}	q_{sc}	η, MeV·zs
5.35	100	0.05	10	0.375	1.20	3.00	1000

4. Numerical fission rates versus the analytical ones

We start from the H-potential (harmonic) which consists of two smoothly matched parabolas with equal stiffnesses $C_{sd} = C_{qs}$. One of the parabolas stretches into the region of $q < 0$. It does not have physical meaning for the fission process, but such potential corresponds best to the assumptions under which Eq. (4) for R_O was derived. The H-potential is shown in Fig. 3 along with the left and right parabolas of which it is constructed. The first suspect in the inaccuracy of the Kramers fission rates is E^*_{tot} or in other words the parameter $\varepsilon = B_f / T$. Therefore we present in Fig. 4 the fractional differences ξ_{IDH} (closed triangles) and ξ_{ODH} (open circles) versus ε.

Since the R_{OH} has been derived from Eq. (3) for the integral Kramers rate R_{IH}, the latter is supposed to agree to the dynamical QSFR better. However, opposite is seen in Fig. 4. This seems to be due to occasional compensation of the inaccuracies made in the derivations of Eq. (4) from Eq. (3). The mutual layout of the ξ_{IDH} and ξ_{ODH} can be explained as follows.

Eq. (4) results from Eq. (3) if one makes an expansion of the potential energy in the exponents up to quadratic terms in $(q - q_{qs})$ and in $(q - q_{sd})$ (the outer and inner integral respectively). In addition, all the upper limits of integration are changed to plus infinity whereas minus infinity is used as the lower limits:

$$R_O = \frac{T}{m\beta}\left\{\int_{-\infty}^{+\infty} \exp\left[-\frac{C_{qs}y^2}{2T}\right]dy \int_{-\infty}^{+\infty} \exp\left[\frac{2B_f - C_{sd}x^2}{2T}\right]dx\right\}^{-1} \tag{5}$$

(note that Eq.(5) holds for all potentials considered in the present work). One can think that the expansion does not change anything for the H-potential since it is made of the two parabolas. It would be so if the integration was performed near the parabolas extremes. However in both integrals, the limits of integration enter the neighbor parabola. Thus both the expansion of the $U(q)$ and the extension of the integral limits matter. The well of the H-potential contains more states than the corresponding left parabola. Therefore $R_{IH} < R_{OH}$ which is seen in Fig. 4.

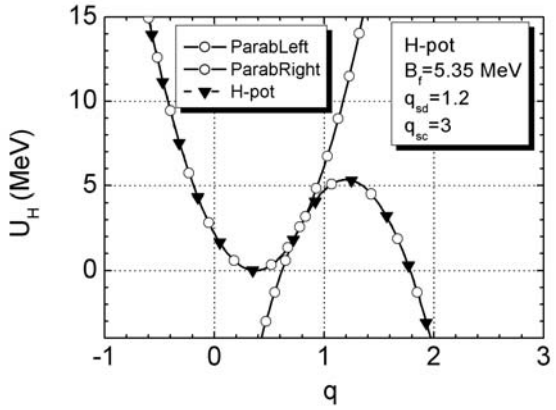

Figure 3. H-potential (closed triangles) along with the left and right parabolas (open circles).

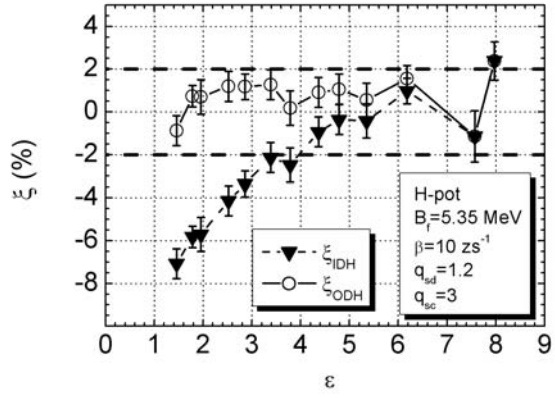

Figure 4. ξ_{ID} (closed triangles) and ξ_{OD} (open circles) versus ε.

Of course the shape of the barrier is not necessarily parabolic. Therefore we have made calculations using the cosine potential (C-potential) of Ref. [13]. The resulting ξ_{ODC} and ξ_{IDC} are shown in Fig. 5 which is analogous to Fig. 4. The ξ_{ODC} is far from zero confirming that the acceptable agreement between R_{OH} and R_{DH} in Fig. 4 was purely accidental indeed.

Eq. (4) accounts only for the two parabolas approximating the C-potential near its extremes. The corresponding upright parabola clearly contains less collective states than the quasistationary well of the C-potential itself. This results in $R_{OC} > R_{IC}$. The inverted parabola presents the barrier which is obviously thinner than the one of the C-potential. This again enhance the R_{OC} in comparison to the R_{IC}. Thus the mutual layout of the R_{OC} and R_{IC} is explained qualitatively.

Comparing Fig. 4 and Fig. 5 we are forced to conclude that the accuracy of Eq. (4) should be taken with care. Moreover only at ε larger than $3.5-4.0$, the R_I agrees to R_D within 2%, essentially like it happens in the case of H-potential.

Of course, the distance between the mass centers of the nascent fragments can not be negative. The potential which accounts for this requirement and keeps the advantages of the H-one, W-potential $U_W(q)$, is again constructed of the two smoothly matched parabolas but is supplemented by an exponential wall preventing Brownian particles to come into the unphysical region $q<0$. When $q>q_{qs}$, the $U_W(q)$ is identical to the H-potential whereas at $q<q_{qs}$ $U_W(q)=C_{qs}\left(q-q_{qs}\right)^2/2+\exp\left(100\left(q_{qs}-q\right)^3\right)-1$. The parabolas on which it is based are the same as in Fig. 3.

Resulting values of the ξ_{ODW} and ξ_{IDW} are presented in Fig. 6. The $R_{IW} > R_{OW}$ and the latter does not agree to the R_{DW} even for $\varepsilon \sim 1$ whereas the R_{IW} reaches the acceptable agreement with the R_{DW} for the values of $\varepsilon > 4$. Opposite to Fig. 5, in Fig. 6 the R_{OW} is smaller than the R_{IW}. This is explained by the larger number of states contained in the upright parabola.

All the potentials considered above were the piece-continuous potentials. Consequently the corresponding forces entering Eq. (1) possess the kinks. One can suspect the kink to be guilty in the inaccuracy of Eq. (4) [14]. Therefore we study one more case corresponding to the polynomial potential of the fifth order (P-potential) which was used in Ref. [15].

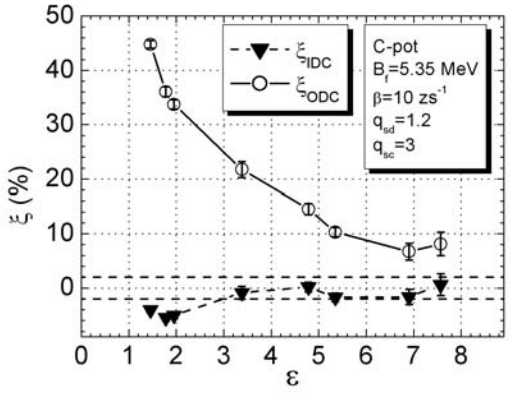

Fig. 5. The same as in Fig. 4 but for the C-potential.

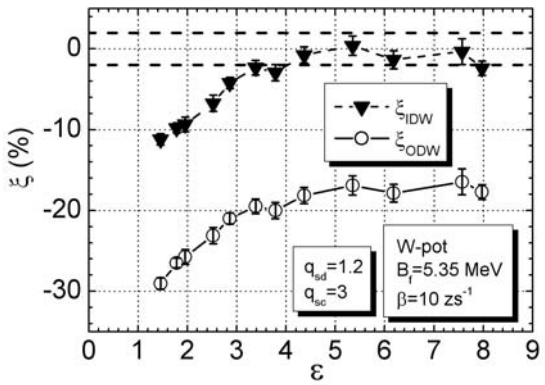

Fig. 6. The same as in Figs. 4, 5 but for the W-potential.

No values of the ξ_{ODP} within 2% is reached in our calculations. Yet the ξ_{IDP} enters the 2% stripe at the same value of $\varepsilon \approx 3.5-4.0$ as in the three previous cases. The qualitative explanation of the relation between the R_{OP} and R_{IP} is literally the same as for the case of Fig. 5.

5. Conclusions

The problem of the accuracy of the Kramers formulas for the fission rate of heated nuclei was not often addressed in the past. Sometimes the difference up to 20% was revealed but the reasons were not identified [4]. Now we have some progress which can be summarized as follows.

The integral Kramers rate of Eq. (3), R_I, agrees with the long time limit of the dynamical rate, R_D, within 2% as the barrier height B_f becomes about 4 times larger than the temperature T. This is to be expected since the accuracy of the Kramers approach is of order of $\exp\left(-B_f/T\right)$. The rate which is obtained from the R_I using the parabolic approximation and the infinite limits for the integrals, R_O, agrees to the R_D only in the case of the two parabolas potential with equal frequencies that allows unphysical negative distance between the fission fragment centers. This happens because of the mutual cancellation of the errors. For the other potentials, the R_O differs from R_D by more than 5% even in the case of $B_f/T > 4$. In particular the $\xi_{OD} = \left(R_O - R_D\right)/R_D$ is about 20% for $B_f/T > 7$ in the case of the W-potential forbidding the negative values of the center of mass distance for future fission fragments. This potential is the closest to the realistic one. The 20% inaccuracy of Eq. (4) is comparable to the quantum, non-markovian and multidimensional effects.

References

[1] Bohr N and Wheeler J A 1939 Phys. Rev. 56 426
[2] Kramers H 1940 Physica 7 284
[3] Fröbrich P and Gontchar I I 1998 Phys. Rep. 292 134
[4] Gontchar I I, Fröbrich P and Pischasov N I 1993 Phys. Rev. C 47 2228
[5] Fröbrich P and Ecker A 1998 Europhys. Jour. D 3 245
[6] Jing-Dong Bao and Ying Jia 2004 Phys. Rev. C 69 027602
[7] Abe Y, Gregoire C and Delagrange H 1986 Journal De Physique 47 329
[8] Fröbrich P and Tillack G-R 1992 Nucl. Phys. A 540 353
[9] Gegechkori A E , Anischenko Yu A, Nadtochy PN and Adeev G D 2008 Phys. At. Nucl. 71 2041
[10] Nadtochy P N, Kelić A and Schmidt K-H 2007 Phys. Rev. C 75 064614
[11] Hofmann H and Ivanyuk F A 2003 Phys. Rev. Lett. 90 132701
[12] Sadhukhan J and Pal S 2010 Phys. Rev. C 81 031602
[13] Edholm O and Leimar O 1979 Physica 98 A 313
[14] Gontchar I I 2008 Proc. of The 2-nd International Conference on Current Problems in Nuclear Physics and Atomic Energy / Ed. by I. M. Vyshnevskyi et al. – Ukraine, Kyiv, 206
[15] Gontchar I I and Aktaev N E 2010 Phys. Rev. C 80 044601